J. Fluid Mech. (1968), *vol.* 32, *part* 4, *pp.* 791–800
Printed in Great Britain

Wave-induced shear instability in the summer thermocline

By J. D. WOODS
Meteorological Office, Bracknell, Berks

(Received 20 October 1967)

The fine structure of the summer thermocline in the Mediterranean Sea around Malta, investigated by a new temperature-gradient meter and by photographs of dye tracers, is summarized. The principal internal feature of the thermocline is a series of thin, laminar-flow *sheets* of high static stability, separated by weakly turbulent *layers* of only moderate density gradient and a few metres thick. A mechanism for generating the patches of turbulence observed on these thermocline sheets is established by comparing dye photographs with a theory by Miles & Howard (1964).

1. Introduction

During the past few years a considerable effort has been directed towards understanding wave motions on the thermocline (e.g. Phillips 1966), but the irreversible processes that accompany its internal evolution have been relatively neglected. The purpose of this paper is to describe the principal fine-scale features of the summer thermocline and to establish, with the help of field observations and a simple theory, one of the major mechanisms by which its structure is controlled.

2. Fine structure of the thermocline

(*a*) *Soundings from the surface*

The classic thermocline model, based on bathythermograph soundings, is illustrated in figure 1, taken from Tully & Giovando (1963). The scale of the smallest features discernible in such plots is limited by the thermal response time of the bathythermograph (Spilhaus 1937). In order to detect still finer structure we used a portable *temperature gradient meter* (Wearden 1966) suitable for sounding to a maximum depth of 50 m from a small open boat. This instrument was used to make spot measurements of temperature (using a single thermistor) and temperature gradient (using two thermistors set 50 cm apart on a vertical fibre-glass rod). The thermistors had a response time of a few tenths of a second and were calibrated to $\pm 0{\cdot}01$ °C: the probe depth was detected by a strain gauge indicator.

Profiles of temperature and temperature gradient were plotted from spot measurements made at 1 m intervals: for convenience, measurements of temperature gradient were made during the probe's descent and temperature during its subsequent ascent. Extra measurements were made in the vicinity of a very

strong temperature gradient to identify the maximum value. A complete sounding took about 15–20 min.

A full description of the fine structure of the thermocline, as determined by this and other instruments, will be the subject of a later publication; here we shall

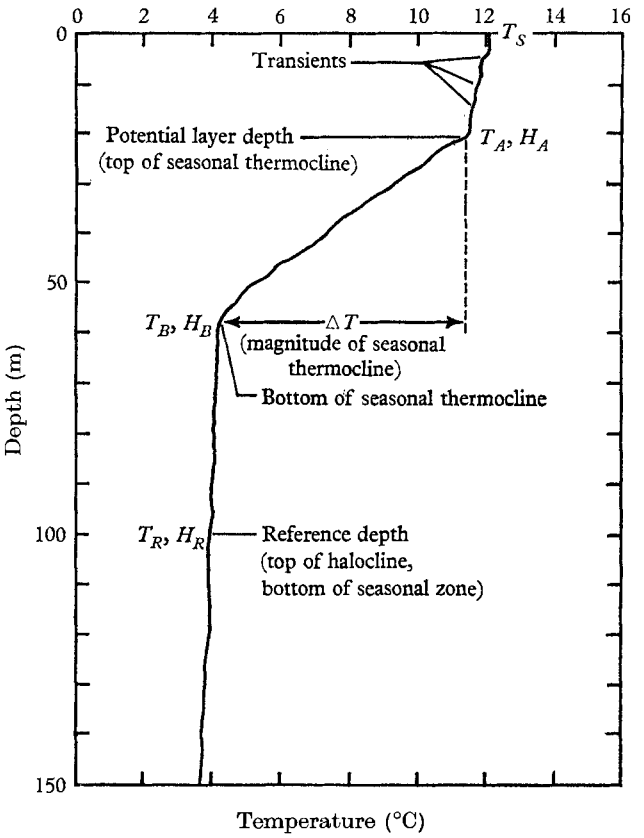

FIGURE 1. The OCEAN model of the summer thermocline (after Tully & Giovando 1963). The resolution of detail within the thermocline is limited by the thermal response time of the bathythermograph.

describe only those features that are relevant to the latter part of this paper. Inspection of a typical sounding (figure 2) shows that the thermocline is divided into several rather thick *layers*, of moderate temperature gradient, separated by much thinner *sheets* of much higher temperature gradient. The horizontal extent of these sheets has yet to be established, but the evidence of (i) repeated soundings at a single, fixed site, and (ii) simultaneous soundings at two separate sites, suggests that individual sheets are at least some tens of miles across. Soundings to 50 m in deep water (2600 m) 100 km east of Marsaxlokk and at our regular site $2\frac{1}{2}$ km east of St Julians (depth 100 m) confirm that this fine structure is typical of the surface layer of the Mediterranean Sea around Malta, and not just a local phenomenon.

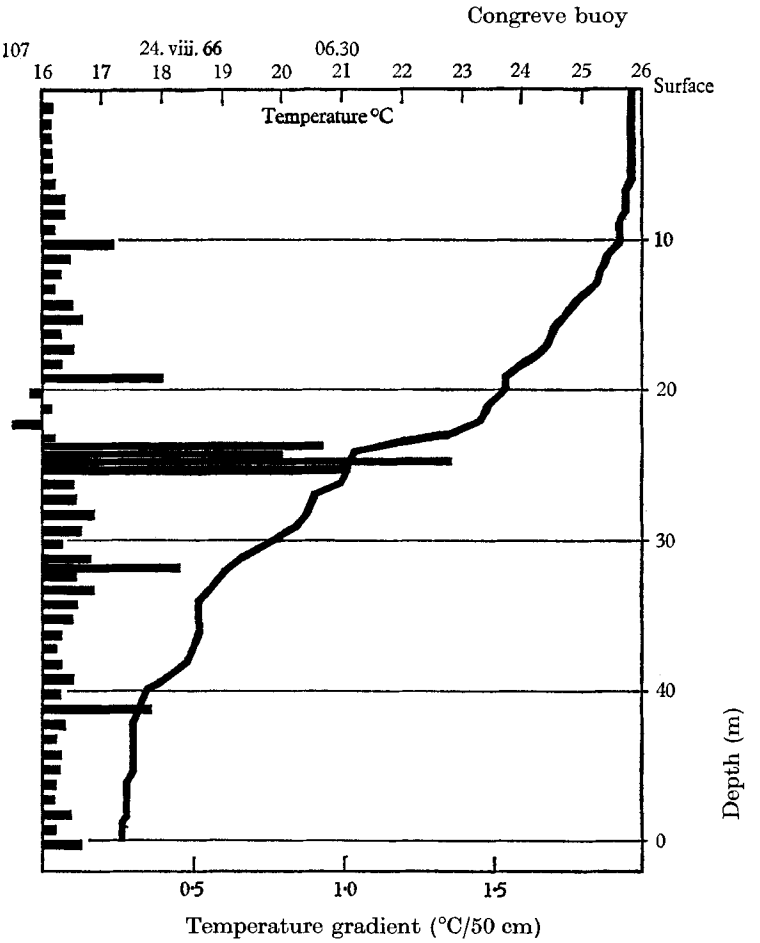

FIGURE 2. Temperature and temperature gradient sounding for 0630/24/8/66. Note the sheets at 10, 19, 24, 32, 41, 50 m. With the exception of the 24 m sheet, these are not resolved by the temperature sounding.

(*b*) *Underwater investigations*

Reports by skin divers (e.g. Linbaugh & Rechnitzer 1955; Banner 1955) suggest that the thin sheets of strong temperature gradient are a common feature of all summer thermoclines. These sheets are often made visible by a marked difference between the refractive indices and turbidities of adjacent layers. In an earlier paper (Woods & Fosberry 1966) we described how dye injected continuously into the sea from a small packet fastened to a fixed vertical line produced a turbulent plume in the layers of only moderate stability, but a broad sheet in regions of very intense temperature gradient. In those sheets the sea exhibited laminar flow; elsewhere it was weakly turbulent. A strong shear was detected across the laminar flow sheets. Later observations confirmed that the laminar sheets seen underwater could always be detected from the surface with the temperature gradient meter.

In order to measure the shear across thermocline sheets we developed a method that had been previously used for demonstration purposes by several workers, notably Lafond (1962). We take a sequence of photographs of the steady distortion of a vertical streak of dye left behind in the wake of a small pellet of soluble

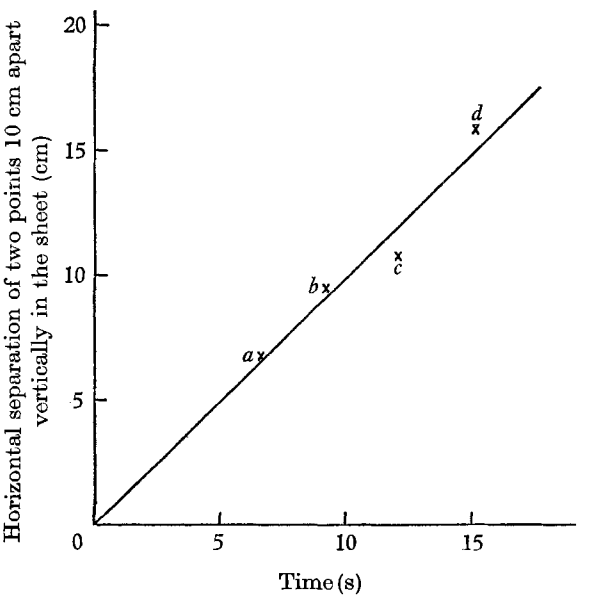

FIGURE 3 (ii) Analysis of figure 3 (i). The shear across the sheet is 0·1 s^{-1}.

fluorescein. This is shown in figure 3 (i), plate 1, where the tiny eddies shed in the pellet's wake are clearly visible. The analysis (figure 3 (ii)) consists of plotting the successive relative positions of pairs of these eddies, which persist as recognizable entities for many minutes in the low ambient turbulence of the thermocline.

This technique may also be used to measure the velocity profile through the whole thermocline: figure 4, plate 1, shows how the current profile is divided into weakly sheared layers separated by strongly sheared sheets.

The shear ($\Delta V/h$) across an individual sheet has variations in time from a minute or so upwards and in space from a few metres upwards. It is convenient, however, to differentiate between the fluctuating 'wave shear' ($\Delta V_w/h$) that can be attributed to an internal wave observed on the sheet, and the much slower changing and more extensive 'drift shear' ($\Delta V_d/h$), although this latter may itself be associated with yet longer waves, which are not detected. Thus:

$$\Delta V = \Delta V_w + \Delta V_d. \tag{2.1}$$

To summarize, the thermocline is divided into half a dozen or so layers of low shear and moderate temperature gradient, separated by thin laminar flow sheets of intense shear and temperature gradient. The precise horizontal extent of these features is uncertain, but it is certainly very much greater than their average spacing of about 4 m. They are found equally over the deep ocean and in relatively shallow coastal waters.

It only remains to add that 'transient thermoclines' which occur sporadically between the surface and the top of the seasonal thermocline (see figure 1) are further examples of *sheets*.

3. Observations of internal waves and breakers

(*a*) *Injection of the dye*

Two methods were used to stain a selected *sheet* with fluorescein dye. The simpler technique involved releasing dye from a single source tied at the appropriate depth to a moored nylon line held taut by a submerged polystyrene float. The dye rapidly becomes distributed within the laminar flow zone by a process similar to that first noted by Taylor (1954) and recently analysed for the sea by Bowden (1965); the shear motions in this case being provided by a combination of (i) the steady relative drift of adjacent layers, and (ii) internal waves (Woods & Fosberry 1966, figure 7).

In an attempt to intensify the coloration of the *sheet* we used a line source consisting of ten dye packets suspended from a horizontal line set orthogonal to the mean drift (figure 5, plate 2). A horizontal view (figure 6, plate 2) shows how thin is the laminar flow zone: the source straddles it, but dye injected into the water above and below rapidly diffuses away into the weakly stable, turbulent water, leaving only that fraction of the dye that became trapped in a region of low (probably molecular) diffusivity. The trapped dye remains visible in the sheet for several hours.

(*b*) *Waves on a thermocline sheet*

The curvature of the dyed sheet seen in figure 5 indicates an internal wave approximately 10 m long and 40 cm high. Coherent trains of such waves, with periods of a few minutes are a regular feature of the thermocline. Being very much shorter than the long waves which move the thermocline as a whole, they affect only a single *sheet*; however, we shall see that they are an order of magnitude longer than the wavelets generated on a *sheet* by shear instability.

An alternative indication of these internal waves is provided by a regular meandering of the dye plume from a point source located near a *sheet* (figure 7, plate 4). This results from either a difference in direction of the quasi steady drift above and below the *sheet* or, less frequently, from a combination of the drift shear with the alternating 'wave shear'.

(*c*) *Wavelets and breakers*

When the dyed thermocline sheet appears (upon even the closest inspection) to be everywhere smooth, then we may confidently state that the flow is laminar and the sheet is *stable*. That is, the static stability of the sheet is sufficient to restrain any instability due to the shear across it at that instant. However, a wave passing over the sheet contributes a further shear, which is strongest at the crest and trough. In some regions this 'wave shear' will tend to cancel the 'drift shear', while in others they will reinforce one another. This may lead to the sheet becoming unstable in discrete patches.

Figure 8, plate 2, shows the first indication of instability on an otherwise stable sheet. As wavelets, about 75 cm in length, begin to form the associated shear motions cause a redistribution of the dye in the sheet, giving bands parallel to the crests and troughs as has recently been observed in tank experiments by Thorpe (1968). These wavelets grow until their height becomes about one-quarter of their length; then they break. Figure 9, plate 2, shows a patch of wavelets and breakers produced by the wave seen edge-on near the top of the picture. The time taken from the first detection of these wavelets until they have completely broken is about 2 min.

Figure 10, plate 3, shows the development of an individual wavelet which, having broken in the classic form described by Rosenhead (1932), throws forward a second smaller breaker. The original breaker was one of a train of four similar wavelets which, like those in figure 8, had a wavelength of about 75 cm, maximum height about 20 cm and a growth time of about 2 min. They were 'triggered' by the wave shown in figure 5, plate 2.

After these wavelets have broken they leave a patch of turbulence which remains active for about five minutes, extracting energy from the shear across the sheet as it is smeared out over the (elsewhere laminar flow) sheet by the steady drift shear. The 'scars' left by these short-lived patches of turbulence persist for several hours, and are a common feature of thermocline sheets (figure 11, plate 4). Turbulent patches have previously been reported by Grant, Moilliet & Vogel (1963) who used a hot wire probe on the prow of a submarine (see also Phillips 1966, p. 188).

4. Theoretical description

(a) *Wavelets*

Miles & Howard (1964) have considered the stability of a thin zone of linear shear and density gradient separating two thick layers of uniform current and density, as shown in figure 12. The Richardson number, J, for this sheet is given by

$$J = gh\Delta\rho/\Delta V^2\rho. \tag{4.1}$$

For a given value of $J < \frac{1}{4}$ the layer will be unstable to disturbances within a specific range of wavelengths, but the fastest growing disturbance will have a length λ_c, given by

$$\lambda_c = 2\pi h/0{\cdot}84 = 7{\cdot}5 \times (\text{thickness of shear zone}). \tag{4.2}$$

Within the range $0{\cdot}05 < J < 0{\cdot}2$, this disturbance will grow exponentially with a scale time τ given very nearly by (4.3) (obtained from Miles & Howard's figure 2)

$$\tau = \frac{1{\cdot}3}{0{\cdot}27 - J} \times (\text{shear})^{-1}. \tag{4.3}$$

(b) *Waves on a density discontinuity*

From Proudman (1953, p. 392) we derive the phase speed, c, of an internal wave of length, λ, on an interface between layers of density and $\rho + \Delta\rho$ moving at V and $V + \Delta V_d$ as

$$c = \left[\frac{g\lambda}{2\pi}\frac{\Delta\rho}{2\rho}\right]^{\frac{1}{2}} - \frac{\Delta V_d}{4}. \tag{4.4}$$

From Phillips (1966, p. 158) we derive a formula for the shear at the crest and trough of an internal wave of length λ, phase speed c and amplitude a on a sheet of thickness h

$$\left(\frac{\partial V}{\partial Z}\right)_{\omega} \simeq \frac{4\pi ca}{h}. \tag{4.5}$$

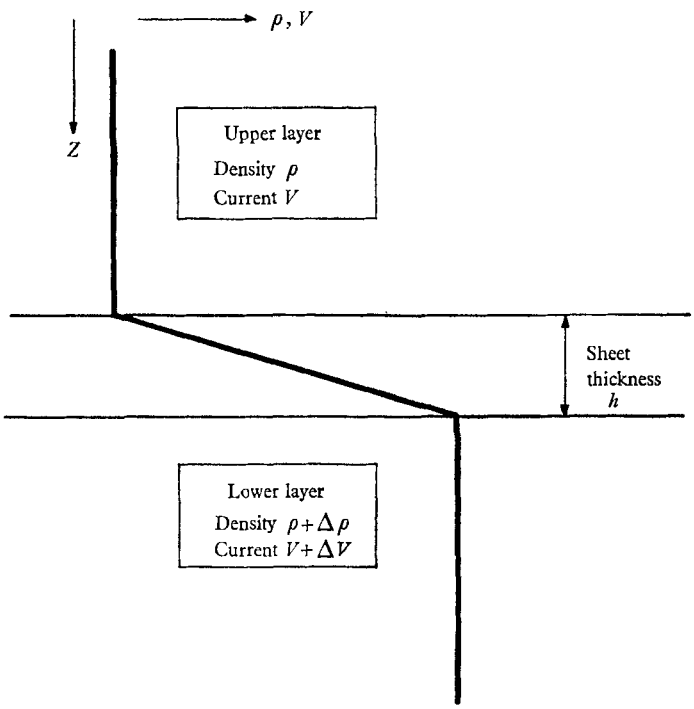

FIGURE 12. Linear shear zone simplifications of a thermocline sheet used when applying Miles & Howard's (1964) theory.

(c) *Comparison with observation*

The wavelets in figures 8, 9, plate 2, and figure 10, plate 3, all had $\lambda \simeq 75$ cm $\pm 10\%$, which implies a shear zone thickness, $h = 10$ cm $\pm 10\%$, which is also the value obtained from figure 3. Clearly then we should not confuse the thickness of the shear zone used to compute the stability of the sheet, with the thickness (< 1 cm) of the laminar flow region lying at its centre.

The temperature difference across the sheet in figure 3 was $\Delta T \simeq 0{\cdot}5$ °C, thickness was $h \simeq 10$ cm and the velocity difference across it was $\Delta V \simeq 1$ cm s^{-1} giving $J = 1$. This is greater than the critical value 0·25, which is consistent with the sheet's observed stability.

The temperature difference across the breakers in figure 9 was 0·4 °C. We have no direct measure of the shear on this occasion, but as the majority of the sheet is stable we may assume that the 'drift shear' is well below the critical value, $(\partial V/\partial Z)_c = 0{\cdot}18$ s^{-1}, that would make $J = \frac{1}{4}$. So the difference in the current speed across the 10 cm thick zone, $\Delta V_d < 1{\cdot}8$ cm s^{-1}.

The extra shear needed to promote the rapid growth of wavelets comes from the long wave visible on the 'horizon' of figure 9: this has wavelength, $\lambda \simeq 10$ m and wave-height $2a \simeq 1$ m. Its speed, calculated from (4.4) is

$$c = 2{\cdot}5 - \frac{\Delta V_d}{4} \text{ cm s}^{-1},$$

i.e.
$$2 < c < 2{\cdot}5 \text{ cm s}^{-1}.$$

The wave shear at crest and trough is given by (4.5),

$$(\partial V/\partial Z)_w = 0{\cdot}15 - 0{\cdot}015\Delta V_d \text{ s}^{-1},$$

i.e.
$$0{\cdot}12 < (\partial V/\partial Z) < 0{\cdot}15 \text{ s}^{-1}.$$

The maximum possible shear at crest and trough is achieved when the wave and drift shear combine: in this example, the total shear cannot exceed $0{\cdot}33$ s^{-1}, which would give $J_{\min} = 0{\cdot}072$. So the minimum possible scale time for the growth of the short waves, given by (4.3), is

$$\tau_{\min} = 20 \text{ s}.$$

This estimate is consistent with the estimated time (~ 2 min) between the initial detection of the short wave and the completion of its breaking, which involves an increase in amplitude by a factor of the order of 20.

Finally it is possible to obtain an independent estimate of the rate of advance of the region of instability from the growth time and wavelength of the wavelets. The distance between the first detectable wavelet and the first completed breaker in figure 13, plate 4, is approximately four wavelengths, so the region of instability is advancing at approximately $2{\cdot}5$ cm s^{-1}. This value, based solely on observation, is in good agreement with the calculated phase speed of the wave ($2 < c < 2{\cdot}5$ cm s^{-1}).

5. Discussion

The examples of sheet instability analysed in §4 were selected largely because clear photographs of them are available for reproduction. However, many other examples were studied during the field work in Malta and these make it possible to indicate the degree of variability experienced in the quoted properties of thermocline sheets. First, it was confirmed, by means of careful soundings with a miniature temperature gradient probe comprising two thermistors set only 10 cm apart, that the temperature profile in the vast majority of sheets follows the velocity profile (figure 3) with, in particular, very sharp (< 1 cm) transitions between the weak temperature gradient outside and the strong temperature gradient inside the sheet. This observation supports the use of the simple sheet model (figure 12) used in §4 and largely removes any ambiguity in deciding the thickness (h) of each sheet. The thinnest sheet observed to become unstable had $h \sim 3$ cm and the largest had $h \sim 30$ cm (figure 14, plate 5), but these were isolated examples; the great majority had a thickness $8 < h < 15$ cm. In all measured cases (including the two extreme ones quoted) the relationship between the sheet thickness h and the wavelength of the instability was within 20% of that ($\lambda = 7{\cdot}5h$) predicted by Miles & Howard (1964).

This paper has been concerned with identifying the instability found on thin sheets in the thermocline; the consequences of this instability will be dealt with in further papers. The first of these (Woods & Fosberry 1967) investigates the effect that the instability has upon the lamination in the thermocline, and shows that if the *sheets* are continually being intensified (i.e. thinned) by entrainment into the adjacent *layers*, then shear instability sets a limit to how thin they can become in a given field of internal waves and drift shear. The next paper (Woods 1968) considers the vertical flux of heat through the thermocline, comparing the heat transferred sporadically through the sheets by the short-lived, but highly conducting patches of turbulence (apertures) caused by shear instability and the far weaker leakage of heat through the remaining laminar flow area of the sheet, with the heat flux through the layers. It is concluded that the vertical heat flux is largely controlled by the frequency of formation of turbulent 'apertures'. Of the papers now in preparation, one will describe how the diurnal heating cycle penetrates the thermocline lamination by provoking extensive shear instability each morning, while another will compare the Kelvin–Helmholtz rolls found in the thermocline with similar rolls in the atmosphere, which have recently been analysed by Ludlam (1967).

This paper is published by permission of the Director General of the Meteorological Office.

The field observations quoted in this paper were made during expeditions to Malta in 1965, 1966 and 1967, supported jointly by the Meteorological Office and the Director of Meteorology and Oceanographic Services (Navy). The author wishes particularly to acknowledge the very considerable assistance afforded him by officers and men of the Mediterranean Fleet Clearance Diving Team and the R.A.F. Marine Craft Unit, Marsaxlokk.

Instruments were kindly made available on loan from the Admiralty Research Laboratory, Teddington, and the National Institute of Oceanography, Wormley.

REFERENCES

Banner, A. H. 1955 Note on a visible thermocline. *Science*, **121**, 402.

Bowden, K. F. 1965 Horizontal mixing in the sea due to a shearing current. *J. Fluid Mech.* **21**, 83.

Grant, H. L., Moilliet, A. & Vogel, W. M. 1963 Turbulent mixing in the thermocline. Pacific Naval Lab. preprint (Esquimalt D.C.) (to be published in *J. Fluid Mech.*).

Lafond, E. C. 1962 Internal waves in *The Sea*, vol. I. Ed. M. N. Hill. London: Interscience.

Linbaugh, C. & Rechnitzer, A. B. 1955 Visual detection of temperature-density discontinuities in water by diving. *Science*, **121**, 395.

Ludlam, F. H. 1967 Characteristics of billow clouds and their relation to clear-air turbulence. *Q. J. Roy. Meteor. Soc.* **93**, 419.

Miles, J. W. & Howard, L. N. 1964 Note on a heterogeneous shear flow. *J. Fluid Mech.* **20**, 311.

Phillips, O. M. 1966 *Dynamics of the Upper Ocean*. Cambridge University Press.

Proudman, J. 1953 *Dynamical Oceanography*. London: Methuen.

Rosenhead, L. 1932 The formation of vortices from a surface of discontinuity. *Proc. Roy. Soc.* A **134**, 170–92.

ROUSE, H. & DODU, J. 1955 Diffusion turbulent à travers une discontinuité de densité. *La Houille blanche* 10e année, pp. 522–9.

SPILHAUS, A. F. 1937 A Bathythermograph. *J. Mar. Res.* (16), 95.

TAYLOR, G. I. 1954 Dispersion of matter in turbulent flow through a pipe. *Proc. Roy. Soc.* A **223**, 446–68.

THORPE, S. 1968 A method of producing a shear flow in a stratified fluid. *J. Fluid Mech.* (in the Press).

TULLY, J. P. & GIOVANDO, L. F. 1963 Seasonal temperature structure in the Eastern Sub Arctic Pacific Ocean, in *Marine Distributions*. Ed. M. J. Dunbar. University of Toronto Press (Canada).

WEARDEN, G. 1966 A temperature gradient meter. (unpublished report). *Admiralty Research Laboratory, Teddington Ref.* 0/30.

WOODS, J. D. 1968 An investigation of some physical processes associated with the vertical flow of heat through the upper ocean. *Met. Mag.* **97**, 65–72.

WOODS, J. D. & FOSBERRY, G. G. 1966 Observations of the thermocline and transient stratifications made visible by dye. In *Malta* '65. *Proc. Symp. Underwater Ass.** (*London*), p. 31.

WOODS, J. D. & FOSBERRY, G. G. 1967 The structure of the summer thermocline, in *Underwater Association Report* 1966–67* (*London*), pp. 5–18.

* Published by the Underwater Association, 181 Gloucester Avenue, London, N.W.10.

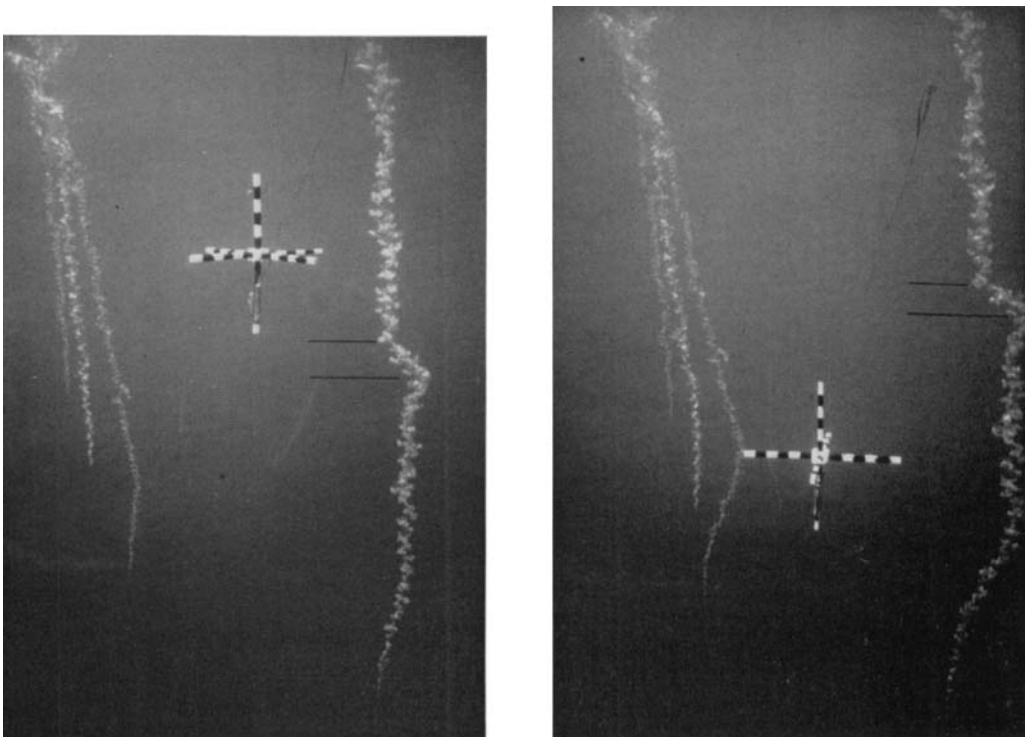

(i, *a*) (i, *b*)

FIGURE 3. (i*a*, *b*) Progressive distortion of a dye streak passing through a sheet. The black and white bands on the scale are 5 cm long.

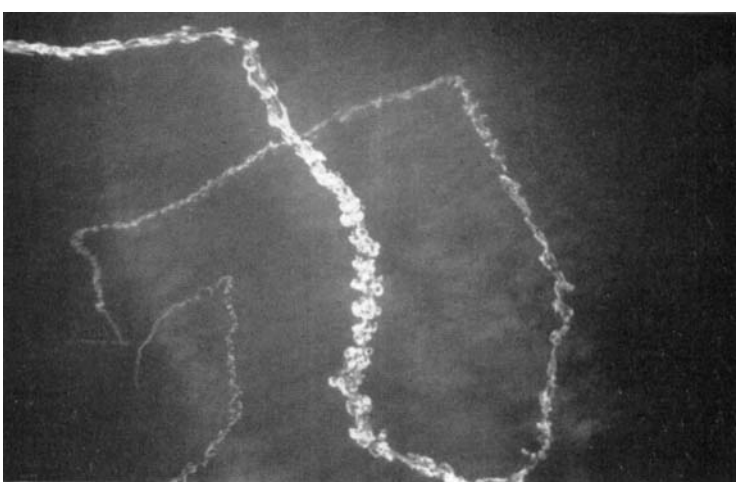

FIGURE 4. The layered structure of the thermocline is illustrated by looking vertically down on to a shear streak, which ends 30 m below the observer.

FIGURE 5. Dye injected into a sheet from a line source consisting of ten packets. Note the internal wave visible on the horizon.

FIGURE 6. Horizontal view of sheet.

FIGURE 8. Dye redistribution on an otherwise evenly dyed laminar flow sheet provides the first indication of wavelets ($\lambda \sim 75$ cm).

FIGURE 9. A patch of wavelets growing to breakers on an otherwise stable sheet ($\lambda \sim 75$ cm.) Note the wave ($\lambda \sim 10$ m, $2a \sim 1$ m) visible on the horizon.

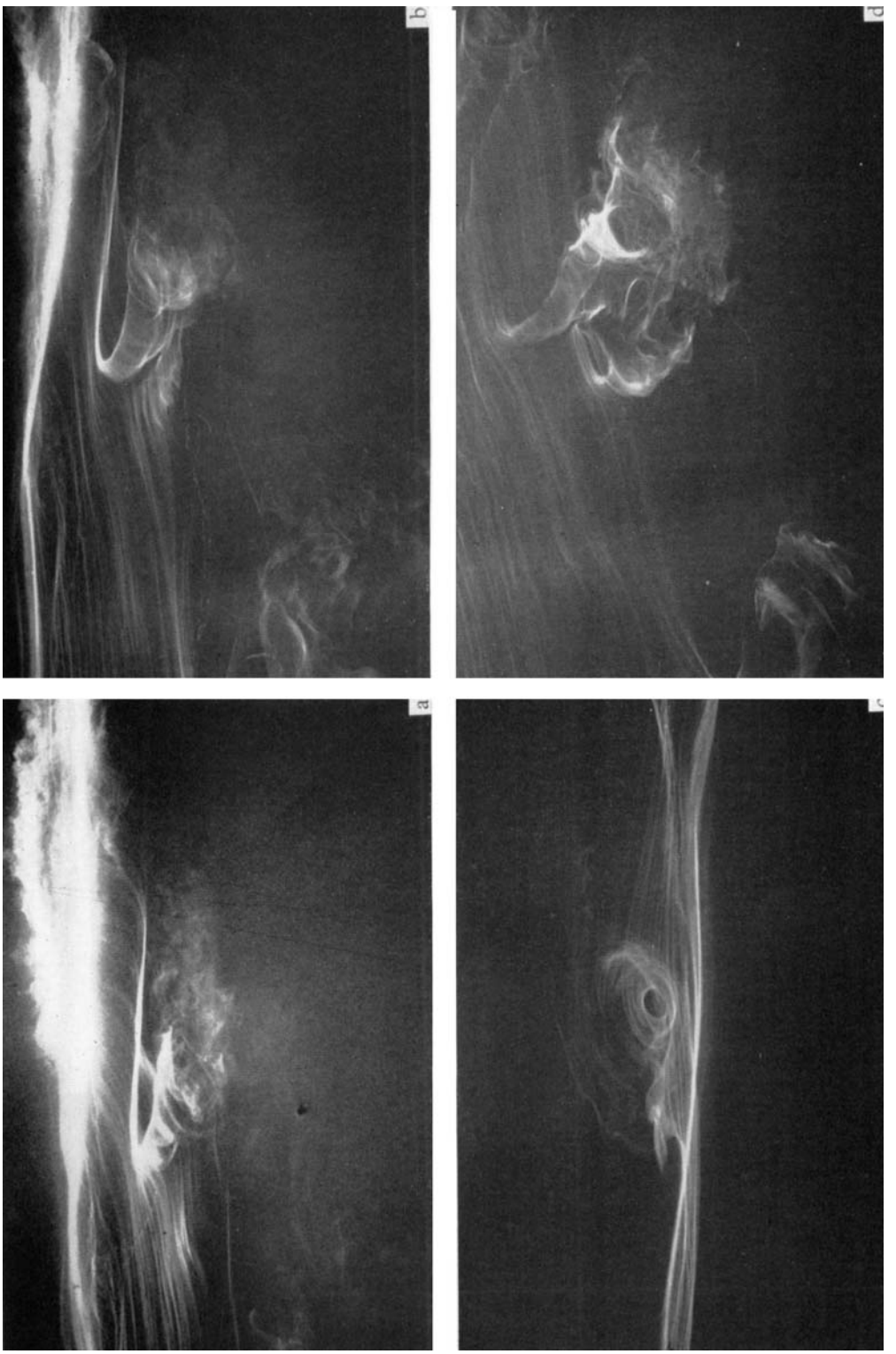

FIGURE 10. The growth of an internal breaker ($\lambda \sim 75$ cm, $2a \sim 20$ cm): (*a*) the initial plunge of the wave crest; (*b*) the complete roll; (*c*) end view of roll showing secondary breaker; (*d*) view from above showing original roll and its secondary, also the neighbouring breakers in the train of four.

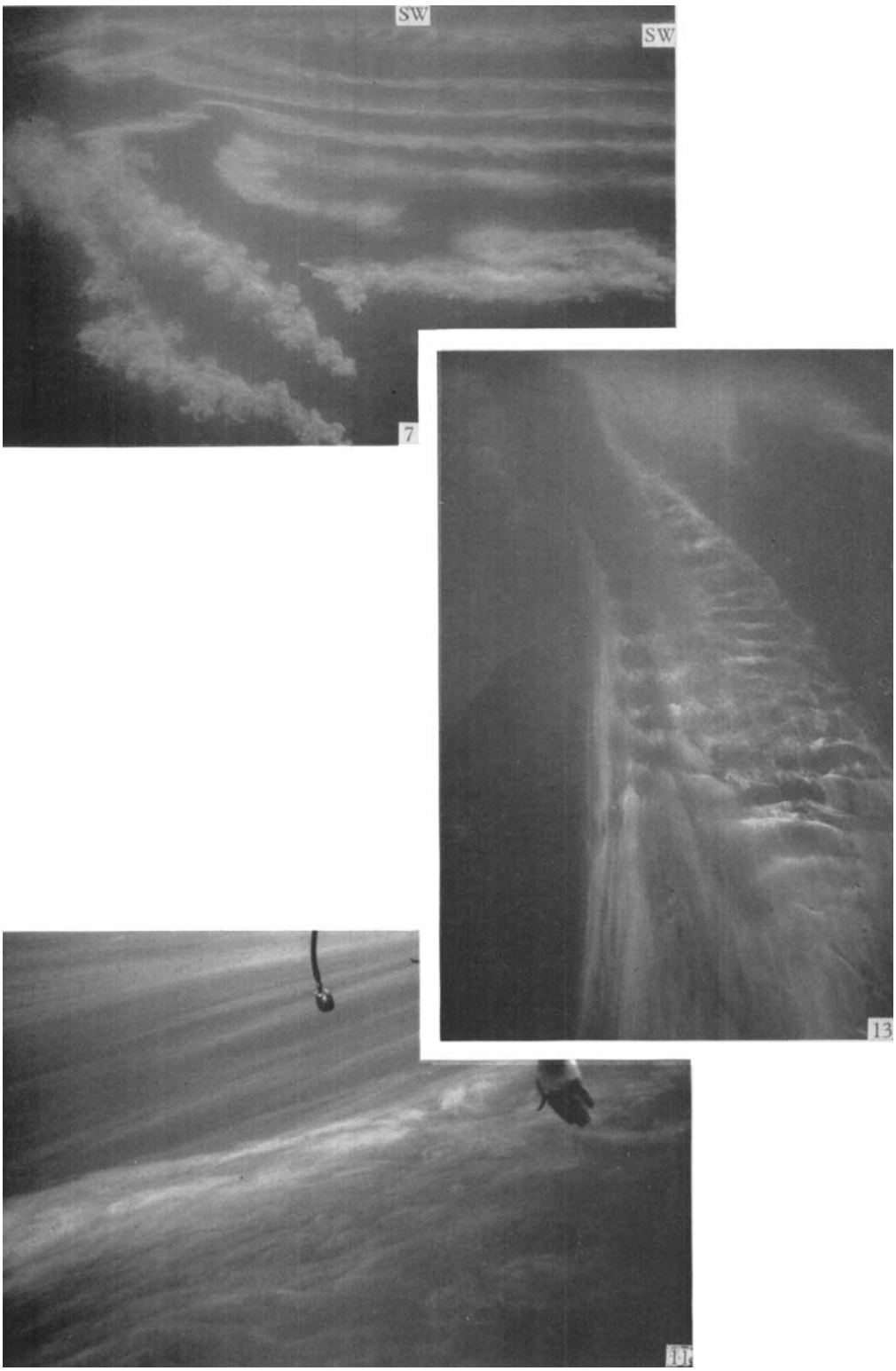

FIGURE 7. Dye plumes from three packets 80 m apart on a vertical line meander in the presence of an internal wave. Note the wavelets (SW) being generated by shear instability near the top of the picture.

FIGURE 11. A 'scar' of mixed water left on a thermocline sheet by turbulence from internal breakers.

FIGURE 13. A patch of wavelets and breakers extending towards the observer at approximately 2·5 cm s^{-1}.

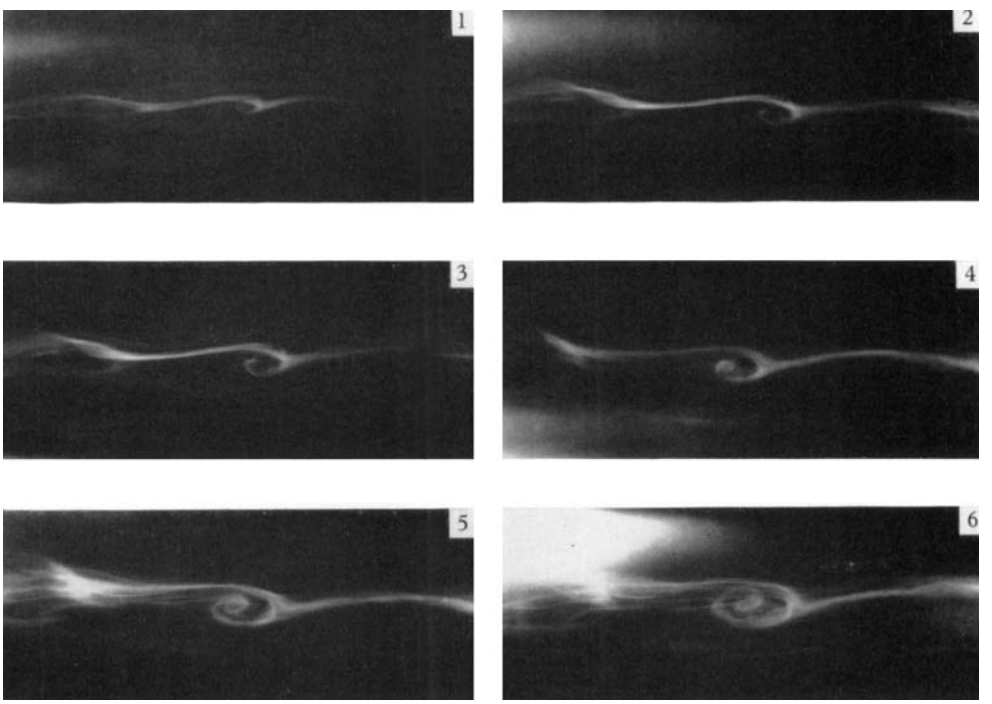

FIGURE 14. Stages in the growth of an exceptionally large breaker (λ, 250 cm; $2a$, 60 cm). Note the 10 cm markings on the scale at bottom right.